

Electrochemical Conversion of CO₂ to Syngas with Controllable CO/H₂ Ratios over Co and Ni Single-Atom Catalysts

Q. He, S. Hwang

To be published in "Angewandte Chemie International Edition"

December 2019

Center for Functional Nanomaterials
Brookhaven National Laboratory

U.S. Department of Energy
USDOE Office of Science (SC), Basic Energy Sciences (BES) (SC-22)

Notice: This manuscript has been authored by employees of Brookhaven Science Associates, LLC under Contract No. DE-SC0012704 with the U.S. Department of Energy. The publisher by accepting the manuscript for publication acknowledges that the United States Government retains a non-exclusive, paid-up, irrevocable, world-wide license to publish or reproduce the published form of this manuscript, or allow others to do so, for United States Government purposes.

DISCLAIMER

This report was prepared as an account of work sponsored by an agency of the United States Government. Neither the United States Government nor any agency thereof, nor any of their employees, nor any of their contractors, subcontractors, or their employees, makes any warranty, express or implied, or assumes any legal liability or responsibility for the accuracy, completeness, or any third party's use or the results of such use of any information, apparatus, product, or process disclosed, or represents that its use would not infringe privately owned rights. Reference herein to any specific commercial product, process, or service by trade name, trademark, manufacturer, or otherwise, does not necessarily constitute or imply its endorsement, recommendation, or favoring by the United States Government or any agency thereof or its contractors or subcontractors. The views and opinions of authors expressed herein do not necessarily state or reflect those of the United States Government or any agency thereof.

Electrochemical Conversion of CO₂ to Syngas with Controllable CO/H₂ Ratios over Co and Ni Single-Atom Catalysts

Qun He,^{†,‡,§} Daobin Liu,^{&,#} Ji Hoon Lee,^{‡,§} Yumeng Liu,[‡] Zhenhua Xie,^{‡,||} Sooyeon Hwang,[§] Shyam Kattel,^{∇,*} Li Song,^{†,*} and Jingguang G. Chen^{‡,||,*}

Abstract: The electrochemical CO₂ reduction reaction (CO₂RR) to yield synthesis gas (syngas, CO and H₂) has been considered as a promising method to realize the net reduction in CO₂ emission. However, it is challenging to balance the CO₂RR activity and the CO/H₂ ratio. To address this issue, nitrogen-doped carbon supported single-atom catalysts are designed as electrocatalysts to produce syngas from CO₂RR. While Co and Ni single-atom catalysts are selective in producing H₂ and CO, respectively, electrocatalysts containing both Co and Ni show a high syngas evolution (total current > 74 mA cm⁻²) with CO/H₂ ratios (0.23–2.26) that are suitable for typical downstream thermochemical reactions. Density functional theory calculations provide insights into the key intermediates on Co and Ni single-atom configurations for the H₂ and CO evolution. The results present a useful case on how non-precious transition metal species can maintain high CO₂RR activity with tunable CO/H₂ ratios.

The extensive consumption of fossil fuels has caused the ever-increasing CO₂ emission, thereby bringing unparalleled and urgent climate problems.^[1] In this regard, many emerging technologies such as sequestration, chemical fixation, and electro/photochemical reduction have been proposed to suppress CO₂ release.^[2] Among these technologies, the electrochemical CO₂ reduction reaction (CO₂RR) has been regarded as a potential route to achieve a net reduction of CO₂ and produce value-added chemicals and fuels when integrated with renewable energy

resources.^[3] To date, many efforts for the exploration of efficient CO₂RR electrocatalysts have been made and various reaction pathways toward not only C₁ products but also multi-carbon products (e.g. C₂H₄, C₂H₅OH, etc.) are well-established. Among the possible products, the production of CO is considered as an attractive approach because CO can be readily utilized as a feedstock for value-added chemicals and fuels via the existing downstream thermochemical reactions.^[3b,4] For these reasons, gold (Au), silver (Ag), zinc (Zn) and palladium (Pd) have been extensively investigated for CO production.^[5]

However, most of the electrocatalysts so far have offered a limited versatility for such a hybrid electro/thermocatalytic process due to the following two reasons. First, their product ratio might not be suitable for the typical syngas (CO/H₂) utilization in the thermocatalytic synthesis as a result of suppressing the hydrogen evolution reaction (HER), which is a major competing reaction of CO₂RR. Second, a high yield production of CO from the dissolved CO₂ remains challenging. Therefore, it is desirable to develop electrocatalysts that can deliver the suitable CO/H₂ ratio with high syngas yield.

In this study, we investigated the earth-abundant 3d transition metal-embedded N-doped carbons (denoted as TM-NC with TM = Co and/or Ni) as CO₂RR electrocatalysts. Through X-ray diffraction (XRD), X-ray absorption fine structure (XAFS), and high resolution electron microscopy analyses, it was confirmed that single TM atom could be effectively anchored into N-doped carbon supports due to the favorable TM-N bond formation, thus enabling distinct CO₂RR behavior from the typical bulk counterparts in terms of the ratio and yield of CO/H₂. In such a single-atom configuration, Ni-NC exhibited an almost exclusive activity to CO evolution (e.g., > 56 mA cm⁻² at 1.0 V vs. reversible hydrogen electrode, V_{RHE}), while Co-NC showed a favorable HER activity (e.g., > 58 mA cm⁻² at -1.0 V_{RHE}). Inspired by this observation, the single-atom catalysts engaging both Co and Ni with different Co/Ni ratios were proposed. The CoNi-NC catalysts maintained the high syngas yield (total current density > 74 mA cm⁻² at -1.0 V_{RHE}) with tunable CO/H₂ ratios (0.23–3.26) suitable for subsequent thermocatalytic reactions. The findings in this study suggest that the choice of TM in a single-atom configuration can be an effective way of tuning the CO/H₂ ratios, thus facilitating the potential adaption of electrochemical CO₂RR to syngas-mediated thermocatalytic processes.

In this work, the N-doped carbon supported single-atom catalysts were synthesized with the method reported previously.^[6] In brief, glucose and dicyandiamide were well-mixed with TM-containing salts in deionized water, followed by evaporating the excess solvent. Then, the obtained powder precursors were annealed at 900 °C to obtain the Co-NC, Ni-NC, and CoNi-NC catalysts. For a control sample, TM-free catalyst was synthesized

^[†] Q. He,^(#) Prof. Dr. L. Song
National Synchrotron Radiation Laboratory, CAS Center for Excellence in Nanoscience, University of Science and Technology of China, Hefei, Anhui 230029, China

E-mail: song2012@ustc.edu.cn

^[‡] Q. He,^(#) Dr. J. H. Lee,^(#) Y. Liu, Dr. Z. Xie, Prof. Dr. J. G. Chen
Department of Chemical Engineering, Columbia University, New York, NY 10027, United States

E-mail: jgchen@columbia.edu

^[§] Dr. D. Liu^(#)
School of Materials Science and Engineering, Nanyang Technological University, Singapore 639798, Singapore

^[||] Dr. Z. Xie, Prof. Dr. J. G. Chen
Chemistry Division, Brookhaven National Laboratory, Upton, NY 11973, United States

^[§] Dr. S. Hwang
Center for Functional Nanomaterials, Brookhaven National Laboratory, Upton, NY 11973, United States

^[∇] Prof. Dr. S. Kattel
Department of Physics, Florida A&M University, Tallahassee, FL 32307, United States
E-mail: shyam.kattel@famu.edu

^(#) These authors contributed equally to this work.

Supporting information for this article is given via a link at the end of the document.

COMMUNICATION

(denoted as NC) with a similar method. Inductively coupled plasma-atomic emission spectroscopy (ICP-AES) measurements were used to analyze the metal contents (**Table S1**) and confirmed that all of the samples have similar metal concentrations (~1.2 wt.%).

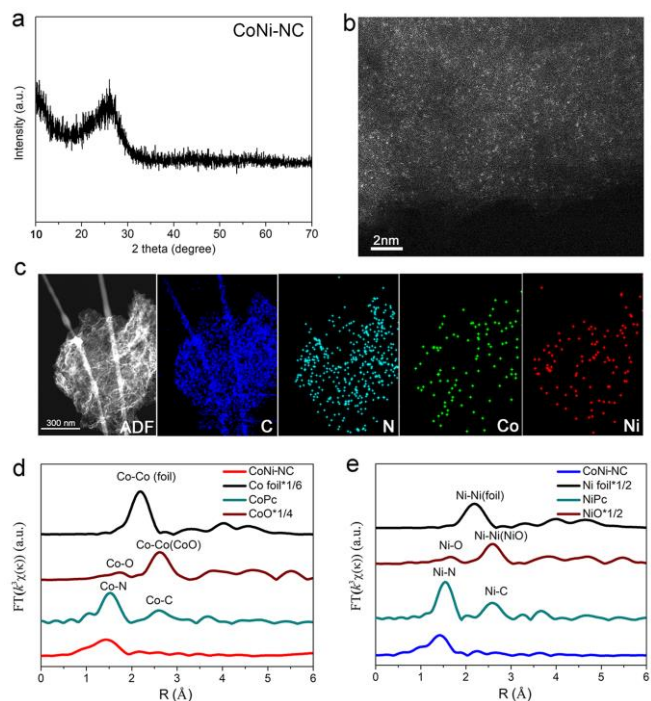


Figure 1. Structural analysis of CoNi-NC. (a) XRD pattern. (b) HAADF-STEM image. (c) Elemental mapping. (d, e) Fourier-transformed (FT) k^2 -weighted EXAFS profiles at (d) Co and (e) Ni K-edge.

The X-ray diffraction (XRD) pattern of CoNi-NC shows a peak around 26° corresponding to the (002) peak of the graphitic array (**Figure 1a**). Its broad peak profile reflects the disordered graphitic stacking along the c-axis and consequently high porosity, which thus helps the isolation of TM on the NC support. This is also in good agreement with the absence of obvious peak of TMs in the XRD profile. A series of catalysts including Co-NC, Ni-NC, and CoNi-NC show similar XRD profiles (**Figure S1**). High resolution scanning transmission electron microscopy (STEM) image also displays an isolated TM environment as shown in **Figure 1b**, **Figures S2a** and **S3a**. The brighter spots indicate the well-isolated TM atoms rather than cluster formation on the NC. Furthermore, the elemental mapping analyses verify the homogeneous distribution of TM over the NC substrate (**Figures 1c**, **Figures S2b** and **S3b**).

It is well-established that single TM atom cannot exist solely on carbonaceous support due to its high surface energy. As such, nitrogen incorporation into a carbon matrix can play an effective role in stabilizing single TM atom via the formation of the TM-N bond.^[7] To verify the chemical information of CoNi-NC, Co-NC, and Ni-NC, X-ray photoelectron spectroscopy (XPS) analysis was carried out (**Figures S4-S6**). XPS survey spectra show the coexistence of TM, N, and C. In the N $1s$ high-resolution spectra, all of the catalysts exhibit four deconvoluted peaks at 398.2 eV (pyridinic-N), 399.7 eV (pyrrolic-N), 401.0 eV (graphitic-N), and 403.3 eV (oxidized-N). Pyridinic-N among these configurations was identified to be one of the dominant N species, which was attributed to the favorable TM-N bond formation.^[8] Such a nitrogen configuration is consistent with the previous reports on

similar single metal-NC catalysts and is also expected to partially oxidize TM through the electron transfer from TM to pyridinic-N.^[9]

To explore the local physicochemical information around TM in TM-NC, X-ray absorption near-edge structure (XANES) and extended X-ray absorption fine structure (EXAFS) analyses were performed.^[10] The XANES profiles of CoNi-NC at the Co and Ni K-edges reveal that the oxidation states of both Co and Ni are between 0 and 2+ (**Figure S7**), implying both TMs are partially oxidized as a consequence of TM-N bond formation. For comparison, Co- and Ni-phthalocyanine (CoPc/NiPc) compounds were measured together due to their similar local structure around TM.^[9] It is worth noting that CoNi-NC shows weakened X-ray absorption peaks at Co and Ni K-edges (dotted circle in **Figure S7**), corresponding to the $1s \rightarrow 4p_z$ transition, than those in Co- and Ni-phthalocyanine (CoPc/NiPc). This transition can be used as a fingerprint for square-planar $M-N_4$ moieties and this intensity reduction thus confirms the distorted D_{4h} symmetry of TM atoms in CoNi-NC.^[9a] The local structural information around TM can be further confirmed from the EXAFS analysis. The Fourier-transformed (FT) k^3 -weighted EXAFS profiles of CoNi-NC at both Co and Ni K-edges show one notable peak around $\sim 1.4 \text{ \AA}$, corresponding to the TM-N bond with a negligible TM-TM interaction in higher R-regions. The peak positions are similar to those of CoPc/NiPc and shorter than those of the TM-O bond in CoO/NiO (**Figures 1d, e**), suggesting that single-atom structure of TM is achieved owing to the presence of metal-N configuration. The Co-NC and Ni-NC are characterized by a similar local structure as CoNi-NC, as suggested by their similar XANES and EXAFS profiles (**Figures S8-S9**). From the combined structural analyses using XRD, STEM, XPS, and XAFS characterization, all of the TM-NC samples in this study most likely possess the single-atom configuration with pyridinic-N coordination.

The electrochemical activity of a series of TM-NC samples toward the CO_2RR was evaluated by using the chronoamperometry method in high-purity CO_2 -saturated 0.5 M potassium bicarbonate (KHCO_3) aqueous solution with vigorous stirring. The obtained gaseous products were quantified by gas chromatography (GC, see the details in Experimental Section). To distinguish the TM single atom from the typical TM nanoparticle (denoted as Co/NC and Ni/NC, **Figure S10**), these catalysts were also tested under the same condition. The representative chronoamperometric current densities at given potentials are presented in **Figure S11**. All of the samples exhibited CO and H_2 as the major gaseous products with the sum of their faradaic efficiency (FE) being near 100% within the potential range in this study.

However, it was revealed that the catalytic conversion of CO_2 -to- CO was significantly affected by the TM choice. For the case of Co-NC (**Figure S12a**), $\text{FE}(\text{H}_2)$ remained almost unchanged near 80% throughout the entire potentials with $\text{FE}(\text{CO})$ being near 20%, with the total current density increasing and reaching $\sim 72 \text{ mA cm}^{-2}$ at $-1.0 \text{ V}_{\text{RHE}}$ (**Figure S12b**). In contrast, Ni-NC was more selective to CO evolution over HER. With increasing overpotential, $\text{FE}(\text{CO})$ was higher than 90% from $-0.5 \text{ V}_{\text{RHE}}$ to $-0.9 \text{ V}_{\text{RHE}}$ and was 86% at $-1.0 \text{ V}_{\text{RHE}}$ (**Figure S13a**). Moreover, Ni-NC showed high $\text{J}(\text{CO})$ values such as $\sim 12.1 \text{ mA cm}^{-2}$ at $-0.7 \text{ V}_{\text{RHE}}$ and $\sim 56 \text{ mA cm}^{-2}$ at $-1.0 \text{ V}_{\text{RHE}}$ (**Figure S13b**), which was better than Au NPs (7.9 mA cm^{-2} at $-0.7 \text{ V}_{\text{RHE}}$) and immobilized Ag NPs ($\sim 8.0 \text{ mA cm}^{-2}$ at $-1.0 \text{ V}_{\text{RHE}}$).^[5c,11] In comparison, both Co/NC and Ni/NC nanoparticle and NC metal-free catalysts exhibited negligible CO_2RR activity (**Figures S14-S16**). Thus, the high partial current

COMMUNICATION

densities observed in TM-NC can be attributed to the optimal utilization of TM due to the single-atom nature of TM.

In order to transform the obtained CO/H₂ into value-added chemicals via conventional thermochemical reactions, their ratio is important because it can control the product compositions.^[12] Therefore, one can conclude that it is beneficial to balance CO₂RR activity and suitable CO/H₂ ratio (0.25~3.3) while increasing the overall CO/H₂ yield for a hybrid electro/thermocatalysis approach.^[12] In this regard, both Co-NC and Ni-NC might not be a good choice because these catalysts would require an additional energy-consuming reactor that provides the missing component, either CO or H₂.

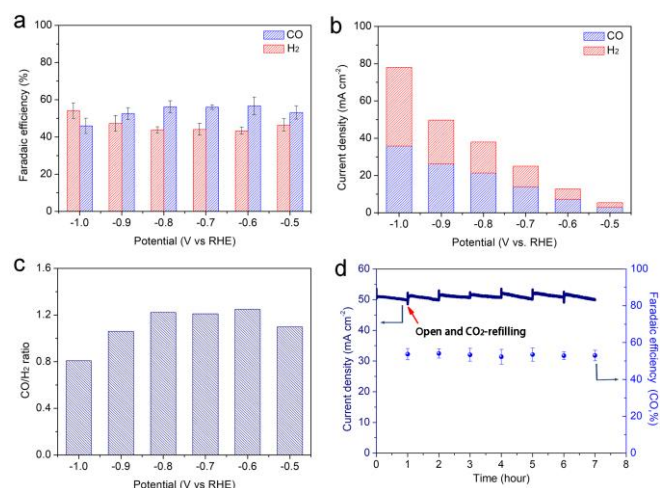


Figure 2. Electrochemical evaluation for CoNi-NC sample. (a) Faradaic efficiencies for CO and H₂ evolution at different potentials. (b) Partial current densities of CO and H₂ evolution at different potentials. (c) Potential dependent CO/H₂ ratios. (d) Long-term stability measured at $-0.9 V_{RHE}$.

To this end, we evaluated CoNi-NC with an equal amount of Co and Ni as a representative bicomponent electrocatalyst. It was revealed that CoNi-NC produced a mixture of CO and H₂ with their FE ranging 45–55% within the potential range applied in the current study (Figure 2a). Moreover, CoNi-NC still maintained the high total current densities (Figures 2b and S17), indicating that the co-existence of Co and Ni did not interrupt the activity of each TM based single-atom catalyst. The CO/H₂ ratios (0.8–1.3, Figure 2c) were in the suitable window of the typical thermochemical process such as Fischer-Tropsch and alcohol synthesis reactions, revealing the promising electrocatalytic properties of CoNi-NC for CO₂RR. Also, CoNi-NC exhibited excellent electrochemical performance (Figure 2d), such a high total current density ($\sim 51 \text{ mA cm}^{-2}$) and favorable FE(CO) of $\sim 53\%$, for 7 h consisting of the repeated 1 h electrolysis at $-0.9 V_{RHE}$, demonstrating promising stability essential for a hybrid electro/thermocatalytic system. Finally, the Faradaic efficiencies and current densities of the main samples at fixed potentials in a longer electrolysis period remained nearly constant, further illustrating the stability of the electrocatalysts (Figure S18).

CoNi-NC catalysts with different Co/Ni ratios (CoNi-NC-*x*, where *x* represents the precursor ratio of Co/Ni. Table S1) were also tested under the same condition. All of these samples exhibited the stable chronoamperometry current density (Figures S19–S20). With increasing Co content, HER became more favorable over CO₂RR while maintaining high total current density, thus enhancing FE(H₂) (Figures S21 and S22). These results imply that varying the Ni and Co ratio in CoNi-NC represents an

opportunity of further tuning the CO/H₂ ratio without sacrificing the high syngas production rate.

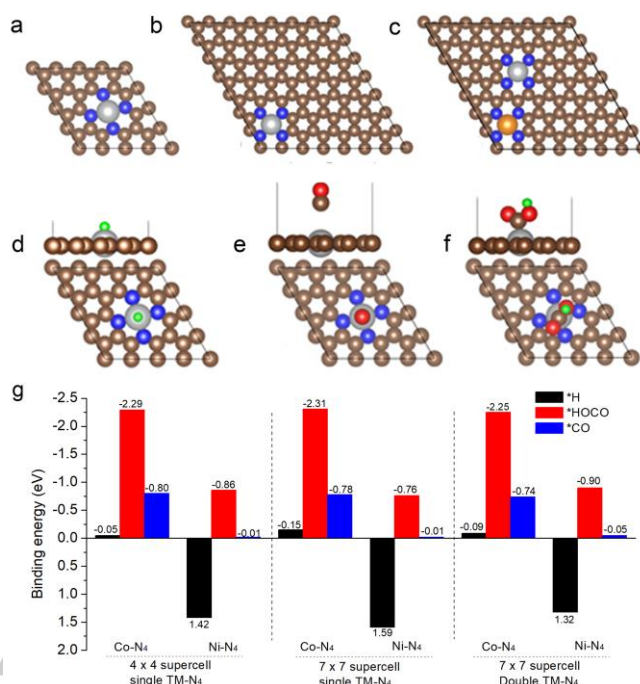


Figure 3. (a–f) DFT optimized structures. (a) Single Ni-N₄ on a 4×4 supercell, (b) single Ni-N₄ on a 7×7 supercell, (c) double Co-N₄ + Ni-N₄ on a 7×7 supercell, (d) *H on Ni-N₄, (e) *CO on Ni-N₄, and (f) *HOCO on Ni-N₄. Ni: gray, Co: gold, C: brown, N: blue, O: red, and H: green. (g) Calculated binding energies (in eV) on TM-N₄/C (TM = Co, Ni) centers.

Density functional theory (DFT) calculations were performed to gain insight into the activity and selectivity of Co-NC and Ni-NC catalysts for HER and CO₂RR. The binding energy of key reaction intermediates *H (for HER), and *HOCO and *CO (for CO₂RR) were calculated on Co-N₄ and Ni-N₄ centers embedded in a 4×4 graphene supercell (Figure 3a), which have been proposed as potential active sites of Co-NC and Ni-NC catalysts, respectively.^[14] Figures 3a–f show the optimized structures of unit cells used in DFT calculations and the energetically most favorable adsorption configurations of the intermediates *H, *CO, and *HOCO on TM-N₄ (TM = Co, Ni) centers. It was found that the reaction intermediates bind at metal sites, indicating that the single metal atoms (e.g. Co and Ni) anchored in graphene plane via N coordination are active centers for catalysis. The DFT calculated binding energies in Figure 3g show that the binding of the intermediates is significantly stronger on Co-N₄ compared to Ni-N₄. Thus, *HOCO formation, a key step/descriptor of CO₂RR,^[15] is facilitated on Co sites compared to Ni sites (Figure S23). However, the strong binding of *CO on Co-N₄ sites (BE = -0.86 eV) makes its desorption, a potential independent step, the rate-limiting step of CO₂RR at all applied potentials on a Co-NC catalyst. On the Ni-N₄ sites, *HOCO formation is predicted to be the rate-limiting step based on the DFT calculated free energy diagrams at a potential $U = 0 \text{ V}$ (Figure S23). The formation of *HOCO is a potential-dependent step and is expected to be facile at an applied external potential. Further, stabilization of *HOCO is expected due to the formation of hydrogen bonding ($0\text{--}0.15 \text{ eV/bond}$) with water molecules at electrochemical conditions.^[16] Finally, the desorption of *CO is predicted to proceed smoothly due to its weaker binding on the Ni-N₄ sites (BE = -0.01 eV). Thus, the DFT results predict that the CO₂RR is facilitated on Ni-N₄

COMMUNICATION

compared to Co-N₄. The binding energy of *H has been identified as a descriptor of HER,^[17] a competing reaction in CO₂RR. **Figures 3g** and **S23** show that the *H adsorption is stronger on Co-N₄ compared to Ni-N₄ and thus the HER should be more favorable on Co-N₄ compared to Ni-N₄. The stabilization of *HOCO under electrochemical conditions should favor the thermodynamics for CO₂RR compared to HER making the Ni-N₄/C sites selective to CO₂RR. In contrast, *HOCO stabilization should not play a role on the Co-N₄ sites for CO₂RR as *CO desorption is predicted to be the rate-limiting step. Overall, in agreement with the experimental measurements, the DFT results predict that Co-NC and Ni-NC should selectively promote the HER and CO₂RR, respectively.

Additional DFT calculations were performed to calculate the binding energies of the HER and CO₂RR intermediates using a 7 × 7 graphene supercell containing both Co and Ni, as shown in **Figures 3b** and **3c**. It was noted from **Figure 3g** that the binding energies of the intermediates calculated on a 4 × 4 supercell are similar to those calculated on a 7 × 7 supercell with one (**Figure 3b**) and two TM-N₄ centers (**Figure 3c**). This suggests that the HER/CO₂RR selectivity of coexisting Co-N₄/Ni-N₄ sites, as shown in **Figure 3c**, is similar to that of single Co-N₄/Ni-N₄ sites shown in **Figures 3a** and **3b**. Thus, consistent with the experimental results, the DFT calculations show that Co-N₄ and Ni-N₄ are predicted to be active sites for HER and CO₂RR when both sites co-exist, which opens up the possibility of tuning the HER/CO₂RR selectivity by changing the Co/Ni ratio.

In order to further highlight the unique CO₂RR properties, a graph of J(CO) versus J(H₂) was constructed for all the TM-NC samples in this study (**Figure S24**). Alongside these data points, we also included data points for other representative electrocatalysts to evaluate the syngas productivity of our samples (**Table S2**).^[5a,5c,5d,13] It can be seen that most of the catalysts, including Ni-NC in the current study, has been investigated to suppress HER. However, despite their high FE(CO), their low J(CO) is still unsatisfactory to provide feedstock molecules to large scale thermochemical syntheses. CoNi-NC shows J(CO) of 36 mA cm⁻² and CO/H₂ ratio of 0.81 at -1.0 V_{RHE}. Such values are remarkable because J(CO) is comparable to or even higher than those of the typical nanostructured catalysts, but is also capable of producing similar J(H₂) at the same time.^[5a,5b,13] Moreover, the CO/H₂ ratio can be easily tunable by simply modifying the Co/Ni ratio in the CoNi-NC catalysts without sacrificing the high syngas yield (**Table S3**).

In summary, we have investigated cost-effective TM-NC samples as CO₂RR electrocatalysts. All of the catalysts exhibited high total current densities, which can be attributed to the single-atom configuration and the consequently optimal TM utilization. In order to tune the CO/H₂ ratios convenient for their utilization in thermochemical reactions, a series of CoNi-NC catalysts, where Co and Ni with different ratios co-existed in a single-atom configuration, were proposed to exhibit controllable CO/H₂ ratios while maintaining high total current densities. This work provides promising catalyst candidates to precious metal-based catalysts for high-yield syngas production with a tunable ratio of CO/H₂, demonstrating the feasibility for potential hybrid electro/thermocatalytic processes for CO₂RR.

Acknowledgements

This work is supported by the US Department of Energy, Basic Energy Sciences, Catalysis Science Program (Grant No. DE-FG02-13ER16381). We thank the Shanghai Synchrotron Radiation Facility (14W1, SSRF) for help in XAFS measurement and Center for Functional Nanomaterials (CFN) for help in characterization (Grant No. DE-SC0012704). S. K. acknowledges computer time allocation (TG-CHE190032) from the Extreme Science and Engineering Discovery Environment (XSEDE) Stampede at TACC, which is supported by National Science Foundation Grant ACI-1548562. L. S. acknowledges the financial supports from National Key R&D Program of China (2017YFA0303500), Q. H. (201806340016) and Y. L. (201806010243) acknowledge financial support from the China Scholarship Council (CSC).

Keywords: CO₂ electroreduction, selectivity control, syngas production, high activity, density functional theory

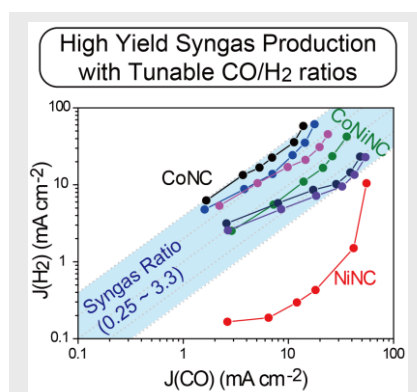
- [1] a) S. Xu, E. A. Carter, *Chem. Rev.* **2019**, *119*, 6631-6669.; b) S. Lin, C. S. Diercks, Y.-B. Zhang, N. Kornienko, E. M. Nicolas, Y. Zhao, A. R. Paris, D. Kim, P. Yang, O. M. Yaghi, C. J. Chang, *Science* **2015**, *349*, 1208-1213.
- [2] a) J. Qiao, Y. Liu, F. Hong, J. Zhang, *Chem. Soc. Rev.* **2014**, *43*, 631-675.; b) P. Gao, S. Li, X. Bu, S. Dang, Z. Liu, H. Wang, L. Zhong, M. Qiu, C. Yang, J. Cai, W. Wei, Y. Sun, *Nat. Chem.* **2017**, *9*, 1019-1024.; c) S. Gao, Y. Lin, X. Jiao, Y. Sun, Q. Luo, W. Zhang, D. Li, J. Yang, Y. Xie, *Nature* **2016**, *529*, 68-71.; d) H. Rao, L. C. Schmidt, J. Bonin, M. Robert, *Nature* **2017**, *548*, 74-77.
- [3] a) Y. Hori, *Modern Aspects of Electrochemistry* **2008**, *42*, 89-189.; b) B. M. Tackett, E. Gomez, J. G. Chen, *Nat. Catal.* **2019**, *2*, 381-386.
- [4] C. Kim, F. Dionigi, V. Beerman, X. Wang, T. Moller, P. Strasser, *Adv. Mater.* **2019**, *31*, 18056175.
- [5] a) J. H. Lee, S. Kattel, Z. Xie, B. M. Tackett, J. Wang, C.-J. Liu, J. G. Chen, *Adv. Funct. Mater.* **2018**, *28*, 1804762.; b) W. Zhu, Y.-J. Zhang, H. Zhang, H. Lv, Q. Li, R. Michalsky, A. A. Peterson, S. Sun, *J. Am. Chem. Soc.* **2014**, *136*, 16132-16135.; c) C. Kim, H. S. Jeon, T. Eom, M. S. Jee, H. Kim, C. M. Friend, B. K. Min, Y. J. Hwang, *J. Am. Chem. Soc.* **2015**, *137*, 13844-13850.; d) D. H. Won, H. Shin, J. Koh, J. Chung, H. S. Lee, H. Kim, S. I. Woo, *Angew. Chem. Int. Ed.* **2016**, *55*, 9297-9300.; *Angew. Chem.* **2016**, *138*, 9443-9446.; e) H. Huang, H. Jia, Z. Liu, P. Gao, J. Zhao, Z. Luo, J. Yang, J. Zeng, *Angew. Chem. Int. Ed.* **2017**, *56*, 3594-3598.; *Angew. Chem.* **2017**, *129*, 3648-3652.
- [6] D. Liu, C. Wu, S. Chen, S. Ding, Y. Xie, C. Wang, T. Wang, Y. A. Haleem, Z. Rehman, Y. Sang, Q. Liu, X. Zheng, Y. Wang, B. Ge, H. Xu, L. Song, *Nano Res.* **2018**, *11*, 2217-2228.
- [7] X.-F. Yang, A. Wang, B. Qiao, J. Li, J. Liu, T. Zhang, *Acc. Chem. Res.* **2013**, *46*, 1740-1748.
- [8] S. Wang, Q. He, C. Wang, H. Jiang, C. Wu, S. Chen, G. Zhang, L. Song, *Small* **2018**, *14*, 1800128.
- [9] a) H. B. Yang, S.-F. Hung, S. Liu, K. Yuan, S. Miao, L. Zhang, X. Huang, H.-Y. Wang, W. Cai, R. Chen, J. Gao, X. Yang, W. Chen, Y. Huang, H. M. Chen, C. M. Li, T. Zhang, B. Liu, *Nat. Energy* **2018**, *3*, 140-147.; b) L. Cao, Q. Luo, W. Liu, Y. Lin, X. Liu, Y. Cao, W. Zhang, Y. Wu, J. Yang, T. Yao, S. Wei, *Nat. Catal.* **2019**, *2*, 134-141.
- [10] K. Jiang, S. Siahrostami, T. Zheng, Y. Hu, S. Hwang, E. Stavitski, Y. Peng, J. Dynes, M. Gangisetty, D. Su, K. Attenkofer, H. Wang, *Energy Environ. Sci.* **2018**, *11*, 893-903.
- [11] Z. Cao, S. B. Zacate, X. Sun, J. Liu, E. M. Hale, W. P. Carson, S. B. Tyndall, J. Xu, X. Liu, X. Liu, C. Song, J.-H. Luo, M.-J. Cheng, X. Wen, W. Liu, *Angew. Chem. Int. Ed.* **2018**, *57*, 12675-12679.; *Angew. Chem.* **2018**, *130*, 12857-12861.
- [12] M. B. Ross, Y. Li, P. D. Luna, D. Kim, E. H. Sargent, P. Yang, *Joule* **2018**, *3*, 257-264.

COMMUNICATION

-
- [13] W. Sheng, S. Kattel, S. Yao, B. Yan, Z. Liang, C. J. Hawxhurst, Q. Wu, J. G. Chen, *Energy Environ. Sci.* **2017**, *10*, 1180-1185.
- [14] K. Jiang, S. Siahrostami, A. J. Akey, Y. Li, Z. Lu, J. Lattimer, Y. Hu, C. Stokes, M. Gangishetty, G. Chen, Y. Zhou, W. Hill, W.-B. Cai, D. Bell, K. Chan, J. K. Nørskov, Y. Cui, H. Wang, *Chem* **2017**, *3*, 950-960.
- [15] J. T. Feaster, C. Shi, E. R. Cave, T. Hatsukade, D. N. Abram, K. P. Kuhl, C. Hahn, J. K. Nørskov, T. F. Jaramillo, *ACS Catal.* **2017**, *7*, 4822-4827.
- [16] F. Calle-Vallejo, J. I. Martínez, J. Rossmeisl, *Phys. Chem. Chem. Phys.* **2011**, *13*, 15639-15643.
- [17] J. K. Nørskov, T. Bligaard, A. Logadottir, J. R. Kitchin, J. G. Chen, S. Pandelov, U. Stimming, *J. Electrochem. Soc.* **2005**, *152*, J23-J26.

WILEY-VCH

High-yield syngas production with CO/H₂ ratio suitable for existing thermochemical syntheses is enabled by tuning single atoms embedded into N-doped carbons.



Qun He,[#] Daobin Liu,[#] Ji Hoon Lee,[#] Yumeng Liu, Zhenhua Xie, Sooyeon Hwang, Shyam Kattel,^{*} Li Song,^{*} and Jingguang G. Chen^{*}

Page No. – Page No.

Electrochemical Conversion of CO₂ to Syngas with Controllable CO/H₂ Ratios over Co and Ni Single-Atom Catalysts